

## Calibration of a detector for nonlinear chromatography

Leonid Asnin<sup>a,b</sup>, Wilmer Galinada<sup>a,b</sup>, Gustaf Götmar<sup>a,b</sup>, Georges Guiochon<sup>a,b,\*</sup>

<sup>a</sup> Department of Chemistry, The University of Tennessee, 552 Buehler Hall, Knoxville, TN 37996-1600, USA

<sup>b</sup> Division of Chemical Sciences, Oak Ridge National Laboratory, Oak Ridge, TN, USA

Received 13 September 2004; received in revised form 23 November 2004; accepted 13 April 2005

Available online 4 May 2005

### Abstract

In many studies of nonlinear or preparative chromatography, chromatographic signals must be recorded for relatively concentrated solutions and the detectors, that are designed for analytical applications and are highly sensitive, must be used under such experimental conditions that their responses are often nonlinear. Then, a calibration curve is needed to derive the actual concentration profiles of the eluates from the measured detector response. It becomes necessary to derive a relationship between the concentration of the eluent and the detector signal at any given time. The simplest approach consists in preparing a series of solutions of known concentrations and in flushing them successively through the detector cell, recording the height of the plateau response obtained. However, this method requires relatively large amounts of the pure solutes being studied and these are not always available or they may be most costly, although these solutions can be recovered. We describe and validate an alternative procedure providing this calibration from a series of peaks recorded upon the injection of increasingly large pulses of the studied compound.

© 2005 Elsevier B.V. All rights reserved.

**Keywords:** Adsorption data; Calibration curve; Detector response

### 1. Introduction

Detector calibration is an important step in nearly all investigations involving nonlinear chromatography because the conventional detectors used in HPLC have been designed to afford high sensitivity responses. Since nonlinear chromatography involves the use of concentrated solutions, detector responses are most often nonlinear in the concentration ranges of interest. Particular problems are encountered in the determination of adsorption isotherms using dynamic methods [1]. The acquisition of accurate adsorption data by frontal analysis (FA) for single components does not require detector calibration, unless the breakthrough curve must be integrated, e.g., when mass transfer resistances are high. With the perturbation method, the elution times of the perturbation signals are the only data needed and a calibration of the detector response is not needed either. When it is possible

to use neither the single-component FA nor the perturbation methods, however, an accurate and adequate calibration curve becomes necessary in order to derive the best values of the isotherm parameters from the experimental data.

To calculate adsorption isotherms using the inverse method or the method of elution by characteristic points, it is necessary to know the dependence of the detector response ( $h(C)$ ) on the concentration of the studied compound in the detector cell ( $C$ ) in order to transform the chromatographic signal from the coordinate system  $h(t)$  into the system  $C(t)$  (where  $t$  is the time). In these investigations, it cannot be assumed that  $h = k C$ , where  $k$  is the detector response constant. In the wide concentration range used in isotherm data measurements, the detector response is almost always nonlinear. Furthermore, at high concentrations, the peak profile itself depends on the sample size, the band width does not remain constant, and its height is no longer simply related to the amount injected. Therefore, detector calibration in preparative chromatography is a more serious problem than the calibration of a detector in conventional elution chromatography.

\* Corresponding author. Tel.: +1 865 974 0733; fax: +1 865 974 2667.  
E-mail address: [guiochon@utk.edu](mailto:guiochon@utk.edu) (G. Guiochon).

In this last case, the area of the elution peak is plotted versus the injected amount of a standard solution and this plot allows the determination of the amount of compound corresponding to any peak, the area of which has been measured. In nonlinear chromatography, we need a calibration curve allowing the back calculation of the concentration of the solution corresponding to a certain signal amplitude. Frequently, this curve is derived from the results obtained in frontal analysis or by merely flushing the detector cell with a series of solutions of known concentrations. However, this procedure wastes large volumes of solvent, requires significant amounts of the pure compound, and it can become quite costly, particularly with synthetic peptides or with many fine organic chemicals.

An indirect method was suggested to derive a calibration curve by adjusting numerically the parameters of a model equation to minimize the difference between the estimated and the known injected amounts of the studied compound [2]. Unfortunately, there are no convenient general equations for this purpose. We report here on a similar method that assumes that the deviations from linear behavior are small.

## 2. Theory

In elution chromatography, the area under the chromatographic peak ( $S$ ) is related to the amount of substance injected into the column ( $q$ ). At low concentrations, this relationship is one of proportionality. When the concentration increases, this relationship deviates from linear behavior, the peak area increasing less and less with increasing sample size because the detector response at high concentrations is no longer linear [3–5]. A proper choice of the experimental conditions (e.g., the selection of a different wavelength in the case of a UV detector) permits a maximization of the dynamic linear range and a minimization of the curvature of the response curve. There are limits to this approach, however. The spectral window of the best diode-array or spectrophotometric UV detectors has a finite width. So, significant deviations from Beer–Lambert law take place whenever the wavelength selected for the measurement of the UV absorbance is not an extremum of the spectrum of the studied compound. Then, the detector response becomes nonlinear in a lower range of absorbance than when the wavelength is selected at a maximum or minimum of the spectrum. This limits the flexibility available in the selection of the observation wavelength. Furthermore, for a variety of reasons, the response ceases to be linear when the absorbance of the solution becomes sufficiently high and a calibration is required whenever the response is not linear. The calibration curve that is needed gives the relationship between the eluent concentration and the detector signal.

A calibration curve relates the response or signal of a detector and the concentration of the studied compound in the detector cell,  $h(C)$ . Hereafter, we will call the inverse function of  $h(C)$ , i.e.,  $C(h)$ , the absolute calibration curve. The relationship between the actual peak area,  $S$ , and the sample

size,  $q$ , will be called the analytical calibration dependence. The function  $q(S)$  is easily measured in conventional elution chromatography, i.e., in analytical applications. In the case of a linear detector calibration, the conversion from  $q(S)$  to  $C(h)$  is easy and straightforward [1,6]. Taking into account that the area under the chromatographic peak in the coordinate system concentration ( $C$ )—volume ( $V$ ) over the interval between the beginning of the peak elution,  $V_1$ , and its end,  $V_2$ , is equal to the amount injected, we have

$$q = \int_{V_1}^{V_2} C(h) dV \quad (1)$$

and one derives that, under linear conditions, we have [6]

$$\frac{1}{k} = \frac{q}{F_v S}, \quad (2)$$

where  $F_v$  is the flow rate and  $1/k$  is the conversion factor in the expression  $C = (1/k)h$ . Thus, in principle, a single analytical injection should be enough in order to obtain the calibration of a linear detector although performing a series of injections in a sufficiently wide sample size range gives better accuracy and precision. One can employ the same approach to determine the absolute calibration curve of a nonlinear detector.

We will assume that the deviation from linear behavior is small, except at very high concentrations. Then, the calibration curve is represented by the following relationship:

$$C = F_1(h) + Kh \quad (3)$$

where  $K$  is a constant and  $F_1(h)$  is the nonlinear term of the calibration equation. Substituting Eq. (3) into Eq. (1) provides the following equation

$$q = \int_{V_1}^{V_2} F_1(h) dV + F_v K S \quad (4)$$

If the absolute calibration function,  $C(h)$ , is nearly linear, the function  $q(S)$  will also be nearly linear. We may rewrite Eq. (4) as the following relationship

$$q = F_2(S) + F_v K S \quad (5)$$

It is obvious that, in order to find the calibration curve, we must solve the following equation

$$\int_{V_1}^{V_2} F_1(h) dV = F_2(S) \quad (6)$$

where  $F_2(S)$  is easily derived from the experimental data afforded by the integration of the elution peaks. In practice, power functions and polynomials are often used to approximate the dependence between  $q$  and  $S$  [3,7,8], although it is possible to use other functions. For the sake of simplicity, we write the nonlinear term as a power term,  $F_2(S) = b_n S^n$ , where  $b$  and  $n$  are numerical coefficients to be determined from experiments. The parabolic dependence is the particular case of the power function with  $n=2$ . In view of the importance of this case we will consider it separately. Taking

into account that  $S = \int_{t_1}^{t_2} h(t) dt$  and  $V = F_v t$ , we must solve the following equation

$$F_v \int_{t_1}^{t_2} F_1(h) dt = b_n \left[ \int_{t_1}^{t_2} h(t) dt \right]^n \quad (7)$$

To solve this equation, it is necessary to know or to assume the form of the function  $h(t)$  describing the profile of the chromatographic peak. The simplest form, one that is often the closest to actual peak profiles, is the Gaussian distribution [9,10]

$$h(t) = H \exp\left(-\frac{t^2}{2\sigma^2}\right) \quad (8)$$

Here  $H$  and  $\sigma$  are the height and the standard deviation of the peak. Obviously, the Gaussian function is only an approximate model of the elution bands observed in liquid chromatography. However, for our purpose, we actually do not need that the peak of the compound studied be retained. Best results will be obtained with a system on which there is no retention but the compound behaves as an unretained tracer. Under such conditions, the main source of band asymmetry is the axial dispersion in the injection system. The exponentially modified Gaussian function is the best model for the bands observed. Since that function would lead us to untractable equations, it is better to operate with a relatively large hold-up volume and a fast injection, leading to only small differences between the actual band used for calibration purpose and the Gaussian curve.

By means of a forward substitution it is easy to show that, in the case of a Gaussian distribution for  $h(t)$ , the solution gives the following absolute calibration curve when the limits of integration are  $(-\infty, +\infty)$ :

$$C = Kh + K_{2,n}h^n \quad (9)$$

where in the general case the constant  $k_{2,n}$  is given by

$$k_{2,n} = \frac{b_n n^{1/2} \pi^{(n-1)/2} 2^{(n-1)/2} \sigma^{n-1}}{F_v} \quad (10a)$$

and, the particular case when  $n=2$

$$k_{2,2} = \frac{b_2 \pi^{1/2} 2\sigma}{F_v} \quad (10b)$$

Obviously, the practical limits of the integration of the signal are the finite times  $t_1$  and  $t_2$  noted earlier but replacing the theoretical integration limits of a Gaussian profile with numerical values that are reasonably practical (e.g.,  $\pm 3\sigma$ ) does not result in any significant numerical error made on the actual peak area [9,10].

The appearance of the peak standard deviation in the formula for the absolute calibration of the detector response arises simply from the choice of the Gaussian equation for the analytical expression that characterizes the shape of the elution bands, because the band width of a Gaussian profile is proportional to its standard deviation. Obviously, if another function (e.g., an exponentially-modified Gaussian equation

[10,11]) were taken as a model for the elution profile of the pulses,  $C(t)$ , the expression for the calibration curve would be quite different. The experimental design used to implement the method should be such that the profile of the pulses entering the detector cell is Gaussian.

In many practical cases, the calibration curve is only slightly nonlinear. Then, the nonlinear term is small compared to the linear one and it is not necessary to estimate it with as high an accuracy as that required for the proportionality constant of the linear part, i.e., the first term in Eq. (9). This assumption allows the use of Eq. (9) even for nearly symmetrical peaks that do not have a strictly Gaussian profile but are characterized mostly by a dispersion parameter because, in this case, the detector signal can be approximated reasonably well with a Gaussian distribution.

Finally, we must underline that the power or the parabolic dependence of the signal on the concentration assumed for the plots of  $S$  versus  $q$  are empirical relationships but other ones could be acceptable as well, depending on the peak shape and on the deviation of the detector response from linear behavior. The use of a suitable polynomial will most often lead to satisfactory results.

### 3. Experimental

#### 3.1. Equipment

All chromatographic measurements were carried out using a HP 1100 liquid chromatograph (Agilent Technologies, Palo Alto, CA) equipped with a column oven, a variable diode-array detector (DAD), a data acquisition system, a computer controller and a manual sample injector, Rheodyne 7725(i) from Rheodyne LLC (Rohnert Park, CA, USA), with a 20  $\mu$ L standard sample loop. The mobile phase flow-rate was kept constant at 1 mL/min in all experiments. The signal of the DAD detector was acquired at a wavelength of 254 nm.

#### 3.2. Materials

The mobile phase was a methanol–water solution (80:20, v/v). Both methanol and water were HPLC grade solvents purchased from Fisher Scientific (Fair Lawn, NJ, USA). The sample component was toluene, also from Fisher Scientific. All chemicals were used as supplied. The column used was a 150 mm  $\times$  4 mm Luna C18 (Phenomenex, CA, USA). During experiments requiring the direct injection of the sample into the detector, the column was replaced by a short piece of a narrow-diameter connector.

#### 3.3. Calibration

In accordance with the theoretical considerations above, the absolute calibration curves were assumed to behave as

either power  $n$  (11a) or parabolic (11b) dependence:

$$C = k_{1,n}h + k_{2,n}h^n \quad (11a)$$

$$C = k_{1,2}h + k_{2,2}h^2 \quad (11b)$$

The coefficient  $k_1$ ,  $k_2$  and  $n$  were considered as either theoretically determined or adjusted parameters depending to the applied method. The expressions relating the amounts injected to the peak area in Eqs. (11a) and (11b), respectively, are given by the following equations:

$$q = F_v K_n S + b_n S^n \quad (12a)$$

and

$$q = F_v K_2 S + b_2 S^2 \quad (12b)$$

### 3.3.1. Indirect methods

The calibration of the detector response using the indirect method was conducted in two modes: with and without column. The evaluation of the calibration curves based on the above-mentioned theoretical approach was done as follows. To determine  $q$  as a function of  $S$  samples of solutions of increasing concentrations, from 0.898 to 81.45 g/L, were injected onto the column with the manual injector. In a second series of measurements, samples of solutions with concentrations increasing from 0.074 to 35.78 g/L were injected into the HPLC system, fitted without a column, and again using the manual injector. Ten data points were acquired for each calibration. Each one of these points is the average of the results obtained for three successive injections. The reproducibility of the peak areas is characterized by a relative standard deviation of 0.5% for the lowest concentration, 0.1% for the highest concentration, with intermediate values for intermediate concentrations. The acquired data were fitted to Eqs. (12a) and (12b) and the best numerical coefficients obtained were used to calculate the calibrating parameters  $k_{2,n}$  ( $k_{2,2}$ ) on Eqs. (10a) and (10b). The parameters of the linear terms in the calibration curves (11a) and (11b) were given as  $k_{1,n}$  ( $k_{1,n}) = K_n(K_2)$  in accordance with description reported in the theoretical section. As the parameter  $n$  in Eq. (11a) was taken the same coefficient of Eq. (12a).

To evaluate the coefficients of the calibration curve using the numerical method described earlier [2], the band profile of the largest sample was transformed into a concentration band profile, using the calibration curve equation and this peak was integrated versus the eluent volume, to obtain an estimated amount of the sample injected for this peak. The parameters values are then adjusted repeatedly using the simplex method [12] to reach the closest possible agreement between the estimated and the known values of the amount injected. It is well known that the simplex method does not necessarily lead to the global optimum but may stop at the closest local optimum, depending on the initial parameter values. Therefore, we examined two sets of initial values:

- the first set was  $k_{1,n}^0(k_{1,2}^0) = K_n(K_2)$ ;  $k_{2,n}^0(k_{2,2}^0) = 0$ ;
- the second set was  $k_{1,n}^0(k_{1,2}^0) = K_n(K_2)$ ;  $k_{2,2}^0(k_{2,n}^0) = k_{2,2}(k_{2,n})$ , derived from Eqs. (10a) and (10b).

The results for each set were compared and the one that gave the smallest discrepancy between calculated and injected amounts was taken to be the best calibration curve conforming to the model equation.

### 3.3.2. Direct method

Direct calibration was finally performed, using the conventional method of filling the detector cell with solutions of known concentrations and measuring the steady-state response of the detector. Seven solutions with concentrations from 0.0266 to 2.858 g/L were used.

## 4. Results and discussion

### 4.1. Calibration from a series of injections

Calibration data obtained by pulse injections into the detector are reported in Fig. 1 (plots of maximum detector signal,  $h$ , versus the amount injected) and Fig. 2 (plots of surface area of a peak versus amount injected). In the case of injections made without column, the  $H$  versus  $q$  plot is more strongly curved and it approaches a horizontal asymptote, showing that we have reached the high limit of sensitivity (maximum absorbance) of the detector. As a consequence, the peak area becomes practically independent of the amount injected, as seen in Fig. 2. The high sample size part of this plot is obviously not suitable for determining a calibration curve. Obviously, the same results can be obtained with either method. However, the band is more disperse at the end of the column, so the results are less sensitive to small fluctuations in the amount injected and are less affected by the response time of the detector. We focused on the investigation of the data obtained with the column.

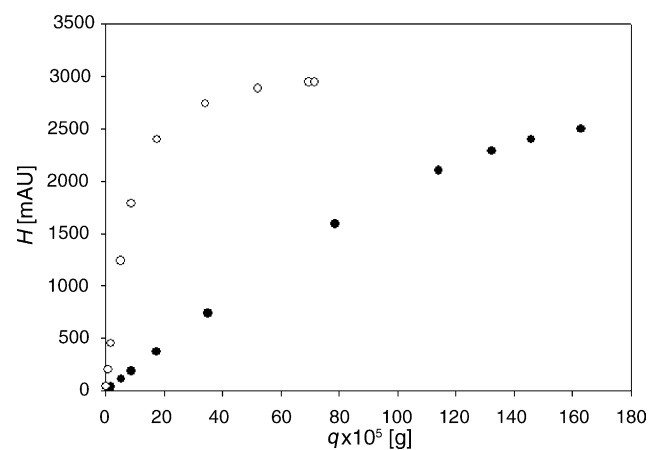


Fig. 1. Height of toluene peak as a function of injected amount. Empty circles—"without column" mode; filled circles—"with column" mode.

Table 1  
Experimental coefficients of Eqs. (12a) and (12b)

	$F_v K_2$	$b_2$	$F_v K_n$	$b_n$	$n$
Value of coefficient	$1.218 \times 10^{-8}$	$4.69 \times 10^{-14}$	$1.235 \times 10^{-8}$	$1.76 \times 10^{-14}$	2.082
Standard deviation	$0.057 \times 10^{-8}$	$0.68 \times 10^{-14}$	$0.16 \times 10^{-8}$	$15 \times 10^{-14}$	0.63

$R^2$  (Eq. (12a)) = 0.9992;  $R^2$  (Eq. (12b)) = 0.9993.

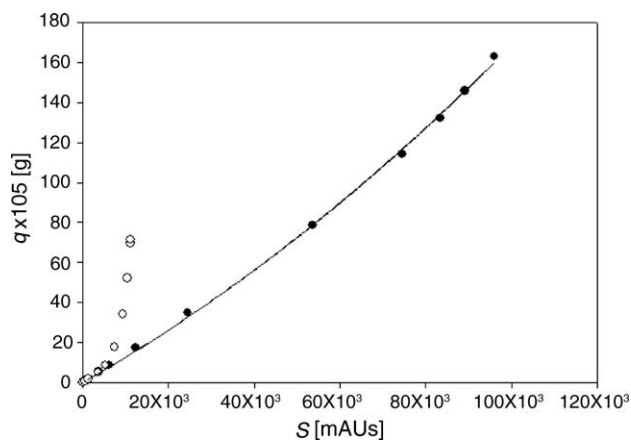


Fig. 2. Injected amount as a function of area of toluene peak. Empty circles—“without column” mode; filled circles—“with column” mode. Solid lines are fit of calibration data with the calibration functions (Eqs. (12a) and (12b)). Note that the parabolic and power functions are superimposed.

Table 1 reports the best values of the numerical coefficients of Eqs. (12a) and (12b) afforded by the nonlinear regression of the data to these equations, the standard deviations of these parameters, and the regression coefficient. The parabolic and the power functions describe the experimental data equally well. The larger values of the standard deviations of the coefficients of Eq. (12a) are explained for the lesser number of its degrees of freedom, not by an actual loss of accuracy compared with that of the parabolic curve. The coefficients of the absolute calibration curves can also be calculated on the basis of the theoretical results derived earlier, assuming that the peak profile is Gaussian (Eqs. (10a) and (10b)). These values are compared in Table 2 with those derived from the chromatographic peak shape and those obtained by the direct method. Since the peak standard deviation depends on the sample concentration (as will be discussed later), we calculated the coefficients of the nonlinear terms for two extreme values of the standard deviation, 0.22 and 0.235.

Table 2

Coefficients of the absolute calibration curves (Eqs. (11a) and (11b)) determined from the shape of the chromatographic peak, calculated by the method proposed, and directly, by frontal chromatography

	Indirect method	Proposed theoretical method		FA	
		$\sigma = 0.220$	$\sigma = 0.235$	Parameter	Standard deviation
$k_{1,2}$	$7.908 \times 10^{-4}$	$7.308 \times 10^{-4}$	$7.308 \times 10^{-4}$	$8.864 \times 10^{-4}$	$0.41 \times 10^{-4}$
$k_{2,2}$	$12.0 \times 10^{-8}$	$1.315 \times 10^{-7}$	$1.405 \times 10^{-7}$	$1.411 \times 10^{-7}$	$0.19 \times 10^{-7}$
$k_{1,n}$	$7.705 \times 10^{-4}$	$7.410 \times 10^{-4}$	$7.410 \times 10^{-4}$	$9.843 \times 10^{-4}$	$0.58 \times 10^{-4}$
$k_{2,n}$	$7.78 \times 10^{-8}$	$6.747 \times 10^{-8}$	$7.247 \times 10^{-8}$	$9.589 \times 10^{-11}$	$68 \times 10^{-11}$
$n$	2.082	2.082	2.082	2.898	0.82

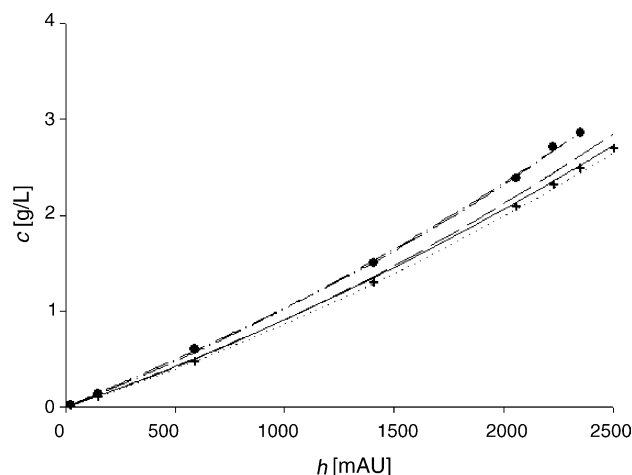


Fig. 3. Comparison of steady-state calibration data (filled circles) and calibration curves determined by numerical indirect method (solid line for parabolic and dashed line for power curves) and the theoretically calculated curves (dotted line for parabolic curve ( $\sigma = 0.22$ ), crosshairs for power curves ( $\sigma = 0.235$ ; see text)). Dash-dot lines are fit of direct calibration data with parabolic and power functions. Note that these parabolic and power curves are superimposed.

Fig. 3 shows the direct calibration curves (concentration versus detector response). The symbols are data points obtained by the classical method of recording the steady signal corresponding to the detector cell filled with a solution of known concentration. The lines are the calibration curves derived using three different methods, using the parabolic (solid line) and the power function (dashed line). The last two lines correspond to the response curves calculated when assuming a Gaussian band profile with standard deviations of 0.22 (dotted line) or 0.235 (cross symbols) and a parabolic response. The corresponding curves calculated for a power response were omitted because they are superimposed with those derived for a parabolic response. All the lines show an excellent agreement. However, the steady-state calibration curve exceeds them by 10–17%.

Table 3

Material balance for peaks estimated with the calibration curves measured by numerical indirect and direct methods

Injected amount ( $10^{-5}$ g)	Amount estimated by numerical indirect method				Amount estimated by FA method			
	Parabolic equation ( $10^{-5}$ g)	$\delta$ (%)	Power equation ( $10^{-5}$ g)	$\delta$ (%)	Parabolic equation ( $10^{-5}$ g)	$\delta$ (%)	Power equation ( $10^{-5}$ g)	$\delta$ (%)
1.80	1.65	-8.1	1.61	-10.3	1.85	3.1	2.05	14.2
5.27	4.99	-5.3	4.85	-7.9	5.59	6.1	6.13	16.4
8.80	8.30	-5.7	8.07	-8.3	9.31	5.8	10.0	13.8
17.45	16.8	-3.7	16.4	-6.0	18.9	8.3	20.2	15.8
35.00	34.8	-0.6	33.9	-3.2	39.1	11.7	40.7	16.3
78.55	83.1	5.8	81.9	4.3	93.8	19.4	94.3	20.1
114.2	121.1	6.1	120.3	5.4	137.0	20.0	137.1	20.1
132.2	138.3	4.6	137.8	4.2	156.5	18.4	156.8	18.6
145.8	149.8	2.8	159.6	9.5	169.6	16.3	170.2	16.7
162.9	162.8	-0.1	162.9	0.0	184.5	13.3	185.5	13.9

 $\delta$  is relative difference between estimated and injected amount.

In Tables 3 and 4 the amounts actually injected are compared with those calculated using the different calibration curves. Regarding the mass balance of the elution chromatograms, the numerical indirect calibration method shows quite good results, the parabolic calibration curve being better than the power one. The theoretically calculated calibration curves give a significantly less good agreement between the actual and the estimated amounts injected than the numerical calibration method at low concentrations but slightly more accurate results at high concentrations. In this case, the power dependence is slightly better than the parabolic one. Differences between the curves calculated for  $\sigma=0.22$  and  $\sigma=0.235$  are not significant. It is interesting to note that the results of this new calibration method are relatively insensitive to small variations of the actual elution profile. However, some strange anomalies are observed. It is probable that a systematic error related to the flow pattern in the detector cell explain some or most of the differences observed in the results delivered by the different methods studied.

#### 4.2. Calibration from a breakthrough curve

The most surprising observation is that the integral mass balance of the peaks is poor when the calibration data derived from the FA data are used. The data lead to a significant

overestimate of the absolute calibration curve, compared with the curve obtained by the indirect method (see Table 3 and Fig. 3). It is possible that the hydrodynamic conditions in the detector cell are different in the elution and the frontal analysis modes. In the FA mode, a solution of constant concentration of the solute flows through the cell, after reaching steady state was reached. The compound concentration is completely homogeneous in the cell. In contrast, in the elution mode, the solute concentration in the mobile phase changes continuously during the elution of a peak through the cell. It is most probably not homogeneous in any radial cross-section. In most cases, as in the present study, this change is fast. It is not sure that the composition of the mobile phase is entirely homogeneous throughout the cell during this elution. Eddies may form, the composition of which lags behind that of the column effluent. Another reason may be a systematic difference between the effects of the manual injection technique used in the elution mode and the procedure employed in frontal analysis. There is little information concerning this possible problem in literature. It has been reported earlier [2], however, that the difference between a steady-state calibration curve and one calculated from the shape of a chromatographic peak amounted to a maximum of about 10%, which is consistent with the results in Fig. 3. Yet, this is a problem deserving of future attention because it is a

Table 4

Material balance of the experimental peaks using theoretical calibration curves

Injected amount ( $10^{-5}$ g)	Parabolic calibration curve				Power calibration curve			
	$\sigma=0.220$		$\sigma=0.235$		$\sigma=0.220$		$\sigma=0.235$	
	$q$ ( $10^{-5}$ g)	$\delta$ (%)	$q$ ( $10^{-5}$ g)	$\delta$ (%)	$q$ ( $10^{-5}$ g)	$\delta$ (%)	$q$ ( $10^{-5}$ g)	$\delta$ (%)
1.80	1.53	-14.8	1.53	-14.8	1.55	-13.7	1.55	-13.7
5.27	4.61	-12.5	4.62	-12.3	4.66	-11.5	4.67	-11.3
8.80	7.70	-12.5	7.71	-12.4	7.76	-11.8	7.77	-11.7
17.45	15.7	-10.0	15.7	-10.0	15.8	-9.5	15.8	-9.5
35.00	32.6	-6.9	32.8	-6.3	32.6	-6.9	32.8	-6.3
78.55	78.9	0.4	79.8	1.6	78.7	0.2	79.6	1.3
114.2	115.8	1.4	117.8	3.2	115.6	1.3	117.4	2.8
132.2	132.6	0.3	134.8	1.9	132.4	0.1	134.6	1.8
145.8	143.9	-1.3	146.3	0.4	143.8	-1.4	146.3	0.4
162.9	156.7	-3.8	159.4	-2.1	156.6	-3.9	159.4	-2.1

Table 5  
Dependence of the characteristics of the toluene peak on the injected amount

Injected amount ( $10^{-5}$ g)	Height (mAU)	$\sigma$ (min)	$2.355\sigma/W_{0.5}$
1.80	37.98	0.218	0.9899
5.27	113.3	0.219	0.9937
8.80	187.0	0.221	1.0057
17.45	372.1	0.220	1.0010
35.00	740.5	0.221	1.0001
78.55	1591	0.223	0.9870
114.2	2103	0.227	0.9460
132.2	2286	0.229	0.9209
145.8	2395	0.231	0.9052
162.9	2499	0.235	0.8932

common practice [1] to postulate the identity of the detector response in the elution and in the FA modes. Admittedly, the numerous examples of successful applications of the inverse method when the necessary calibration curves were measured by the steady-state technique [11,13] suggest that the systematic error that this assumption may entail is not very large. An error of about 10% is not inconsistent with this observation.

Compliance of the peak profile with the assumption of a Gaussian distribution is important in the theoretical derivations. We also assumed that the standard deviation of the sample peak is constant. However, the experimental data (Table 5) show that  $\sigma$  increases with increasing injected amount, although this variation is negligible. A 100-fold increase of  $q$  causes only a 7% increase of  $\sigma$ . The deviation of the peak profile from a Gaussian distribution was evaluated from the ratio  $2.355\sigma/W_{0.5}$  (with  $W_{0.5}$ , the peak width at half-height), which is equal to 1 for a Gaussian peak. Deviations from the Gaussian shape are noticeable for  $q = 78 \times 10^{-5}$  g and reach 11% for  $q = 162.9 \times 10^{-5}$  g. However, it is worth noting that these deviations did not lead to any serious error on the mass balance. Also, changing the value of  $\sigma$  from 0.22 to 0.235 does not change significantly the estimate of  $q$ . This is because the linear term of the calibration function (Eq. (9)) is much larger than the nonlinear one. For the largest amount injected ( $162.9 \times 10^{-5}$  g) the ratio of the linear and the nonlinear terms is about 2.7.

## 5. Conclusions

The theoretical approach delineated earlier allows the determination of the absolute calibration curve of a detector from its elution peaks when these peaks have a Gaussian

or a nearly Gaussian profile. The accuracy of the results of this method is comparable to that of a numerical indirect method also described in this paper. Further development of this method would require the solution of Eq. (7) in the case of peaks of arbitrary shape, taking into account the possible dependence of parameters characterizing the peak profile on the injected amount. The surprising observation that there is a small but significant difference between the absolute calibration curves determined by the steady-state method (i.e., from the FA concentration plateau heights) and by the new method based on the area of pulse injections should be further investigated. Since it is probably due to differences in the flow pattern in the detector cell in FA and in elution chromatography and since we studied only the Agilent DAD detector, similar investigations will be carried out using UV detectors manufactured by other companies and other types of detectors.

## Acknowledgments

This work was supported in part by Grant CHE-02-44696 of the National Science Foundation and by the cooperative agreement between the University of Tennessee and Oak Ridge National Laboratory.

## References

- [1] A.V. Kiselev, Ya.I. Yashin, Gas-Adsorption Chromatography, Plenum Press, New York, 1969.
- [2] E.V. Dose, G. Guiochon, Anal. Chim. 62 (1990) 816.
- [3] P.W. Carr, Anal. Chem. 52 (1980) 1746.
- [4] C.D. Pfeiffer, G.R. Larson, J.F. Ryder, Anal. Chem. 55 (1983) 1622.
- [5] T.E. Beesley, B. Buglio, R.P.W. Scott, Quantitative Chromatographic Analysis, Marcel Dekker, New York, 2001.
- [6] C.F. Poole, The Essence of Chromatography, Elsevier, Amsterdam, 2003.
- [7] L. Kirkup, M. Mulholland, J. Chromatogr. A 1029 (2004) 1.
- [8] S. Héron, M. Dreux, A. Tchaplá, J. Chromatogr. A 1035 (2004) 221.
- [9] N. Dyson, Chromatographic Integration Methods, Royal Society of Chemistry, Cambridge, UK, 1990.
- [10] A. Felinger, Data Analysis and Signal Processing in Chromatography, Elsevier, Amsterdam, 1998.
- [11] A. Felinger, A. Cavazzini, G. Guiochon, J. Chromatogr. A 986 (2003) 207.
- [12] M.A. Sharaf, D.L. Illman, B.R. Kowalski, Chemometrics, Wiley, New York, 1986.
- [13] F. Gritti, G. Guiochon, J. Chromatogr. A 1033 (2004) 43.